

Coherent Mott Excitations Captured on the Timescale of Electron Correlations

S. Wall^{1#}, D. Brida^{2#}, S. R. Clark^{3,1}, H.P. Ehrke^{1,4}, D. Jaksch^{1,4}, A. Ardavan¹,
S. Bonora², H. Uemura⁵, Y. Takahashi⁶, T. Hasegawa⁷,
H. Okamoto^{5,6,7}, G. Cerullo², A. Cavalleri^{1,4*}

¹*Department of Physics, Clarendon Laboratory, Oxford UK*

²*Dipartimento di Fisica, Politecnico di Milano, Italy*

³*Centre for Quantum Technologies, National University of Singapore*

⁴*Max Planck Research Group for Structural Dynamics, University of Hamburg-CFEL*

⁵*Department of Advanced Materials Science, University of Tokyo, Japan*

⁶*Photonics Research Institute, AIST, Tsukuba 305-8562, Japan*

⁷*CREST-JST, Kawaguchi 332-0012, Japan*

By using nearly-single-cycle optical pulses in the near infrared, we measure the time-dependent optical properties of the Mott insulator ET-F₂TCNQ after prompt photo-excitation. We observe a rapid drop in spectral weight at the Mott gap, and oscillations in the optical conductivity, revealing coherent electronic-structural rearrangements on the timescale of electron correlations. A quantum dynamic model based on the Fermi Hubbard Hamiltonian predicts recurrence oscillations between bound and unbound holon-doublon pairs, closely matching the experimentally observed frequency. To date, coherent many body processes of this kind have only been experimentally accessible in ultracold gases, where the correlation energies are re-normalized to lower values and the dynamics is correspondingly slower. We bridge the gap between optics on extreme timescales and the control of strongly correlated quantum gases, and identify the first steps in the coherent response of a Mott insulator.

Mott insulators are fractionally filled solids whose electrons are made immobile by their mutual repulsion. If the on-site Coulomb energy U is large compared to the single-electron hopping amplitude t , charges localize and the material does not conduct. Characteristically, Mott insulators are very sensitive to doping. If a fraction of the sites are emptied, and electron-lattice coupling is weak, the balance can be easily tipped in favour of the competing tendency of electrons to de-localize and minimize their kinetic energy. A filling-controlled insulator-metal transition ensuesⁱ.

These characteristics are conceptually different from those of conventional band insulators, in which mutually independent electrons do not conduct at the Fermi wavevector owing to Bragg scattering from the lattice. In a band insulator, the electronic properties are determined by lattice symmetry, and doping alone does not alter the electronic structure.

The filling-controlled insulator-metal transition in a Mott insulator is usually studied by chemical doping, i.e. by comparing the static properties of different crystals with varying densities of impurities. However, this makes it often difficult to distil the physics of electrons from the physics of other strongly coupled degrees of freedom, which may also rearrange when the density of dopants is changed. For example, trapping and de-trapping of charges by lattice distortions, enhanced scattering, or unwanted perturbations in magnetic order, may accompany chemical substitution. In this context, photo-doping with short pulses of light is an alternative strategy to study the physics of filling control in stoichiometrically pure compounds, offering a new way to manipulate their collective state and also to understand correlated electron physics dynamically and out of equilibrium.

ET-F₂TCNQ, bis(ethylenedithio)-tetrathiafulvalene-difluorotetracyanoquinodimethane, is a stacked molecular solidⁱⁱ, in which ET acts as a donor and F₂TCNQ as acceptor molecule (Figure 1). The electronic properties are dominated by the ET molecules, which lose one electron per site to the F₂TCNQ molecules and form half-filled, narrow bands. Conducting electrons are localized due to the large on-site Coulomb repulsion ($U \sim \text{eV}$), which substantially exceeds the single electron hopping amplitude ($t \sim 0.1 \text{ eV}$)ⁱⁱⁱ. The system is a Mott insulator, exhibiting no lattice distortion even at low temperatures. As shown in

figure 1, light polarized parallel to the a axis of the crystal is strongly absorbed only for photon energies above the Mott gap at $E_M = 0.7$ eV. This sharp feature corresponds to inter site transitions $(ET^+, ET^+) \rightarrow (ET^{2+}, ET^0)$ i.e. transitions between the lower and upper Hubbard bands. The narrow bandwidth of ET-F₂TCNQ is also clearly seen in the dielectric function and optical conductivity.

Upon doping, one expects the system to become conducting, resulting in two main changes of the optical properties. Recently, it has been shown that photo-excitation^{iv} across the Mott gap can transiently generate a metallic state in ET-F₂TCNQ. This was evident from the short-lived, Drude-like response at long wavelengths, reflecting the existence of mobile carriers and, most importantly, a reduction in Mott gap resonance at 0.7 eV. However, the 100-fs temporal resolution of these experiments prevented the observation of the dynamics on the fundamental timescales set by the electron correlations.

The non-equilibrium rearrangements in the electronic structure of Mott insulators are dictated by the energy scales of electron hopping and their correlations. If $t \sim 0.1$ eV, as in ET-F₂TCNQ, we expect hopping among two sites to require tens of femtoseconds ($\hbar/t \sim 40$ fs, where \hbar is Planck's constant). Similarly, for correlation energy on this scale, we expect a similar quasi-particle formation times, or "dressing" time of a bare electron^v.

To observe dynamics in this regime, it is then necessary to impulsively photo-excite the system and probe its response with a time-resolution equal to or better than 10 fs. Excitation must also be tuned to 0.7 eV (1.7 μ m) Mott gap, in order to minimize the effect of hot electron relaxation. This has not been possible to date, due to the lack of an optical device that generates sufficiently short pulses in the infrared. At the infrared wavelengths required for this experiment, the period of the light is approximately 5 fs, which makes it very challenging to generate pulses in the sub-10 fs region. To this end, we developed a new optical parametric amplifier, in which pulses are compressed to durations of less than two optical cycles with an adaptive pulse shaper based on a deformable mirror^{vi}.

In Figure 2, we report a time-resolved reflectivity measurement of the photo-induced response of ET-F₂TCNQ, in its paramagnetic, Mott insulating phase at room temperature. The sample was excited with a 9-fs pulse around the 1.7 μm gap, and the time-dependent reflectivity changes recorded with an Optical Multi-channel Analyzer for each time delay. The essential features observed in our ET-F₂TCNQ experiments are reported in figure 2. Immediately after photo-excitation, a prompt drop in the reflectivity at the Mott gap is observed, indicative of the loss of spectral weight and collapse of the gap. Relaxation back to the Mott ground state occurs with a bi-exponential decay with 300-fs and 1.35 ps time constants.

To put this observation in context, we note that dynamics observed here is unique to a Mott insulator with weak electron phonon coupling. Solids with strong electron lattice coupling, such as K-TCNQ^{vii,viii}, VO₂^{ix}, or compounds exhibiting Charge Density Wave ground states^x, show slower dynamics limited by the rearrangement time of the lattice distortions, and formation of metastable phases that relax to the ground state only after several nanoseconds.

In the lineouts of figure 2, we also show a fit (red curve) of the reflectivity spectrum at all time delays, based on a multi-Lorentzian model of the frequency dependent dielectric function. Starting from this fitting procedure, we extract the time dependent optical conductivity at each time delay associated with the Mott gap, shown in the colour plot in the upper right side of figure 3. The time dependent conductivity follows the same qualitative features observed in the time dependent reflectivity.

The most striking observation emerges by analysing the transfer in spectral weight of the optical conductivity, which can be seen clearly in a second colour plot in figure 3 (lower right), where we show the time dependent conductivity normalized to the maximum value at each time delay. Oscillatory shifts in the central wavelength can be clearly seen, with a period of nearly 40 fs and strong damping. These oscillations are markedly different to those caused by coherent phonons, which modulate the amplitude of the reflectivity at the

phonon frequency^{xi}, which is not observed here. A coherent electronic process is thus strong candidates to explain the physics observed here.

To describe these observations, we used a one dimensional Fermi Hubbard Hamiltonian for a half-filled, ten-site chain, with transfer integral t , onsite interaction U and nearest neighbour interactions V ,

$$H = -t \sum_{l,\sigma} \left(c_{l,\sigma}^\dagger c_{l+1,\sigma} + c_{l+1,\sigma}^\dagger c_{l,\sigma} \right) + U \sum_l n_{l,\uparrow} n_{l,\downarrow} + V \sum_l n_l n_{l+1}$$

with periodic boundary conditions. The terms $c_{l,\sigma}^\dagger$ and $c_{l,\sigma}$ are the creation and annihilation operators for an electron at site l with spin σ , and $n_{l,\sigma} = c_{l,\sigma}^\dagger c_{l,\sigma}$ is the number operator at site l with spin σ . Since ET-F₂TCNQ is a Mott insulator with no spin ordering at room temperature ($T_N \sim 40$ K), we described the state of the unperturbed solid by the density matrix $\rho_g = \frac{1}{2^N} \sum_{\sigma_T} |\psi_{\sigma_T}\rangle \langle \psi_{\sigma_T}|$, which is a statistical mixture of all possible spin configurations with one electron per site with each configuration having an equal probability. Strictly unitary filling with a mixed spin configuration comes from the fact that the room temperature energy scale is significantly higher than J and significantly lower than U . Thus, ρ_g has effectively infinite spin temperature and zero charge temperature. Each $|\psi_{\sigma_T}\rangle$ represents a many-body wavefunction with one electron per site and total spin configuration σ_T . The index N represents the total number of sites, which for the calculations reported here was restricted to ten.

Using ρ_g as the initial state of the system, we calculated the unequal-time current-current correlation function as $c_{jj}(T) = \text{tr}[\rho j(T)j(0)]\theta(T)$ where j is the current density, T is

time, $j = it \sum_{l,\sigma} (c_{l,\sigma}^\dagger c_{l+1,\sigma} - c_{l+1,\sigma}^\dagger c_{l,\sigma})$, and $\theta(T)$ is the Heaviside function centered at $T = 0$.

The Fourier transform of the current-current correlation function was then used to calculate the optical conductivity as a function of frequency.

U , V and t were varied in order to fit the static optical conductivity, using a scaling constant A to calculate its absolute size in the appropriate units. The best fit to the static optical properties, shown in the lineouts of figure 3 ($\tau = -200$ fs), gives $U \sim 800$ meV and $V \sim 100$ meV and $t \sim 50$ meV, comparable to experimental estimatesⁱⁱⁱ. Importantly, it was not possible to fit the optical conductivity using U and t alone, and a sizeable intersite correlation energy V , was required to fit the line shape of the peak .

To analyse the time-dependent conductivity of figure 3, we used the model described above, and we separated the dynamics into two regime. One regime, considered the incoherent recovery of the Mott state and is dominant after several hundreds-of-femtoseconds and can be considered a population dynamic. The second consisted of the coherent dynamics created by the laser pulse which occur at early time delays and requires a complete quantum description.

We first discuss the incoherent dynamics, modelling the loss of spectral weight, red-shift of the conductivity and its recovery at longer times. We consider the states created by the laser to be of the form $\rho_{e,L} \propto X_L^\dagger \rho_g X_L$, where X_L is an excitation operator of the form,

$$X_L = \sum_{\sigma, l=1}^L \left(c_{l,\sigma}^\dagger c_{l+1,\sigma} + c_{l+1,\sigma}^\dagger c_{l,\sigma} \right)$$

The summation runs over all spin configurations, labelled by σ . This excitation operator creates a coherent superposition of delocalized neighbouring pairs of holes and doubly occupied sites, on top of the spin mixed background ρ_g and corresponds to the transfer of 1 across the Mott gap for every 10 ET molecules. In a one dimensional system, this type of excitation is referred to as a holon-doublon pair. When $L=10$ the excitations are completely delocalized though-out the system, and at $L=1$, the excitations are localized on a specific site.

To reproduce the time dependent optical conductivity $\sigma(\omega, \tau)$ at long time delays, where τ is the time delay between the pump and probe beams, the system was described by an incoherent mixture of the two states $\rho(\tau) = p_g(\tau)\rho_g + p_e(\tau)\rho_{e,L=1}$, i.e. only a combination of the initial and a state with a localized holon-doublon pair. The optical conductivity, $\sigma_{e,1}(\omega)$, of the state $\rho_{e,L=1}$ was calculated with same parameters of U , V , and t as the initial state. The time dependant optical conductivity can then be expressed as $\sigma(\omega, \tau) = p_g(\tau)\sigma_g(\omega) + p_e(\tau)\sigma_{e,1}(\omega)$, where $p_g(\tau)$ and $p_e(\tau)$ represent the time-dependent fraction of the sample in each state at time τ . The optical conductivity was fitted by find the values of p_g and p_e as a function of time with the constraint $p_g(\tau) + p_e(\tau) = 1$. This procedure, which neglects any interference between the states, gave an increasingly satisfactory fit for delays longer than 200 fs. The red curve in the lineouts of figure 3 (upper left) shows the good matching between the measured conductivity and the fit.

This model could not be used to describe the oscillatory response observed at the earliest time delays, for which the quantum coherent properties are not negligible. To simulate the quantum-coherent dynamics immediately after excitation, we considered an excited state $\rho_{e,L=10}$ chosen to model the system immediately after photo-doping at $\tau = 0$, a delocalized holon-doublon state, which was chosen to be coherent over all simulated sites (length $L = 10$). This excited state was then allowed to freely evolve according to the Fermi Hubbard Hamiltonian and at each time delay the optical conductivity was calculated. Again, the values of U , t and V used were the same as those derived from the fit of the static optical conductivity, and the calculation was performed with no free parameters. The normalized result of this simulation is shown in the color-coded plot in figure 4, correctly reproducing the initial red shift and a 25-THz oscillatory response of the optical conductivity.

In absence of a detailed description of the optical field, the absolute amplitude of the shifts was not faithfully predicted, but the key feature observed in the experiments, the 25-THz spectral oscillations of the conductivity, was reproduced well. The Fourier transforms of simulated and measured response are shown in the upper right panel of figure 4. In

addition, no damping of the system was considered, which allows the system to continue to oscillate for many cycles.

The physical origin of the observed oscillations can be intuitively understood as follows. Laser excitation promptly creates holon-doublon pairs, which in the first instance occupy neighboring sites $|\dots1\mathbf{0}\mathbf{2}11\dots\rangle$, where $\mathbf{0}$ and $\mathbf{2}$ denote holon and doublon, and the sites indicated as 1 are singly occupied. This excited state involves a repulsive interaction U on the doublon site and an attractive interaction $-V$ between the holon and the doublon. This many-body excited state is also coupled by a finite hopping amplitude t to another state in which holon and doublon are non-adjacent $|\dots1\mathbf{0}\mathbf{1}\mathbf{2}\mathbf{1}\dots\rangle$. These two states energies differ by the intersite correlation energy V (see figure 4).

The underlying physical picture is perhaps most transparent when pictorially represented as a single particle problem, in which each site is represented by a quantum well. Adjacent doublon states are offset by an energy V (depending on their distance to the holon) and are coupled by the hopping t (see figure 4). In this simplified case, one would expect coherent oscillations in the occupancy to occur with Rabi frequency $\Omega = \sqrt{V^2 + t^2}/\hbar$, corresponding to oscillations between a bound and free holon doublon pair. For the parameters used here $\Omega = 27$ THz, in excellent agreement with our measured frequency.

In our discussion so far, we have not explored the origins of the decay back to the ground state. The data shows a rapid loss of coherence due to coupling to other degrees of freedom, and a recovery of the integrated spectral weight within approximately one picosecond. It is interesting to compare this latter observation to recent experiments performed in an optical lattice for a fermion gas at ultracold temperatures. That experiment identified a decay of excited doublons through purely electronic channels^{xii}. It was found that the doublon decay time scales exponentially as U/t . Although the dimensionality of the system it is remarkable that the predicted decay time, of order several hundred femtoseconds, is the same order of magnitude as the fast decay found in our experiment.

In summary, by using nearly single cycle optical pulses in the infrared, we have captured the first step in the excitation of a Mott insulator with light. By comparing our experiments to a quantum dynamic model, we have unveiled coherent recurrences between bound and ionized holon-doublon pairs. It is remarkable that the Fermi-Hubbard model, with parameters derived from near-equilibrium fits can quantitatively describe important aspects of the physics far from equilibrium. By considering other strongly correlated electron materials, such as ones in which Fermi-Hubbard physics gives rise to unconventional superconductivity, the larger bandwidths and higher correlation energies imply that many processes of interest will become observable only on even shorter timescales, approaching the attosecond regime^{xiii}. We anticipate that time resolved photo-electron spectroscopy^{xiv} as well as ultrafast soft x-ray techniques^{xv} will play a major role in these studies. Our experiments, which explore physics that to date has only been accessible in ultracold gases^{xvi,xvii}, open the way to coherent spectroscopy and manipulation of many body physics in real materials at high temperatures.

FIGURE CAPTIONS

Figure 1: Cartoon and optical properties of the crystal structure of ET-F₂TCNQ, bis(ethylenedithio)-tetrathiafulvalene-difluorotetracyanoquinodimethane. ET acts as a donor and F₂TCNQ as acceptor molecule. The electronic properties are dominated by the ET molecules, which form half-filled bands. The system is a Mott insulator, and conducting electrons are localized, due to the large on-site coulomb repulsion ($U \sim \text{eV}$), which exceeds the electron kinetic energy, $t \sim 0.1 \text{ eV}$. The experimental reflectivity is also displayed. Real part of the dielectric function ($\text{Im}[\sigma]/\omega$) and real part of the optical conductivity, extracted from the reflectivity by Kramers Kroenig transformation.

Figure 2: Time dependent optical reflectivity of ET-F₂TCNQ. **Upper panel:** The changes in the spectrally integrated reflectivity are reported, showing the collapse of the correlation-gap and its rapid recovery. **Lower Panel:** In the two-dimensional colour plot, the time-dependent reflectivity is shown for the spectral region between 1.2 μm and 2 μm .

Figure 3: **Upper left:** Spectral lineouts of the time dependent optical conductivity of ET-F₂TCNQ in the spectral region between 1.2 μm and 2 μm . **Upper right:** Colour coded conductivity as a function of time and wavelength. **Lower left:** Picture of the unitary filled ground state ρ_g and of the excited state ρ_e displaying a holon-doublon pair. **Lower right:** In the lower right panel the normalized optical conductivity is shown for the first 150 fs, with oscillations in spectral weight with a period of approximately 40 fs. The fit to the time dependent lineouts using a theoretical model of the optical conductivity are shown in the left hand side.

Figure 4: **Upper left:** Calculated time dependent evolution of the conductivity by considering the quantum coherent evolution of the state ρ_e (see figure 2). **Upper right:** The experimental and theoretical Fourier transforms are compared in the upper right plot. **Lower left:** Cartoon of the different configurations for an Mott insulator. Two states

differing by onsite interaction energy V and coupled by tunnelling amplitude t give rise to the high frequency oscillations in the spectral weight. **Lower right:** Intuitive representation based on a single view of the physics. The cartoon maps the two excited states onto bare states of a double-well potential, coupled by t and with energy offset V . The cartoon also shows the probability distribution of the lowest energy eigenstates.

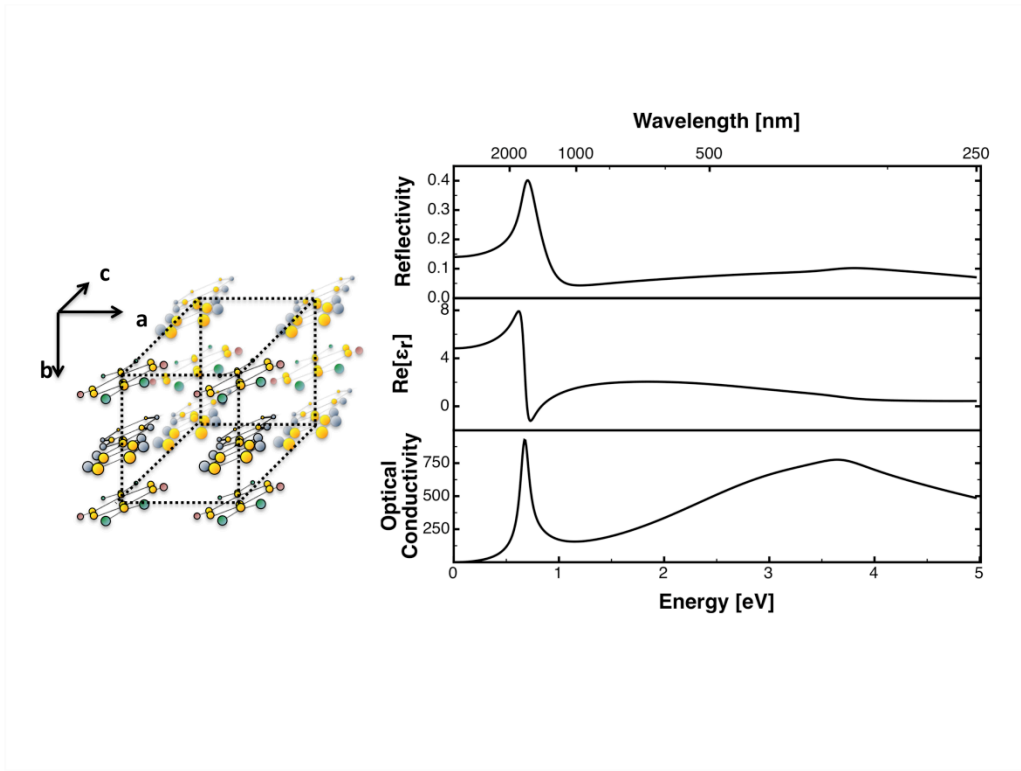


Figure 1

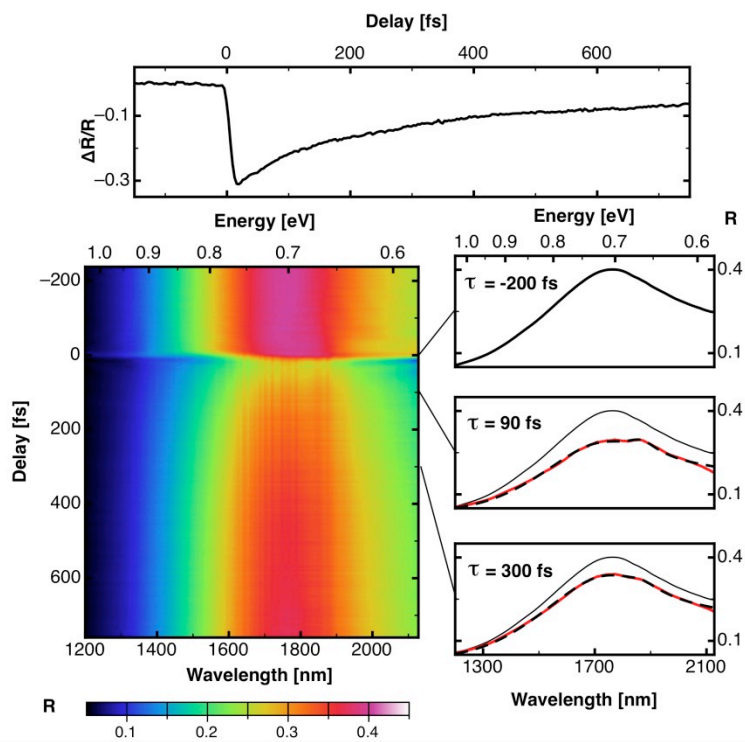


Figure 2

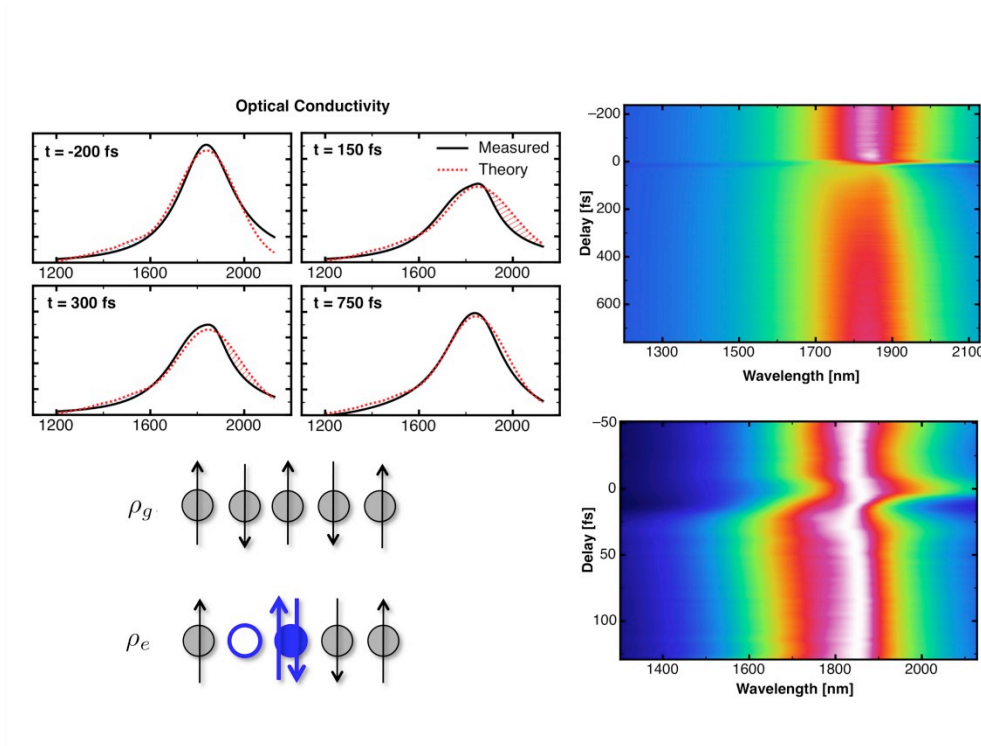


Figure 3

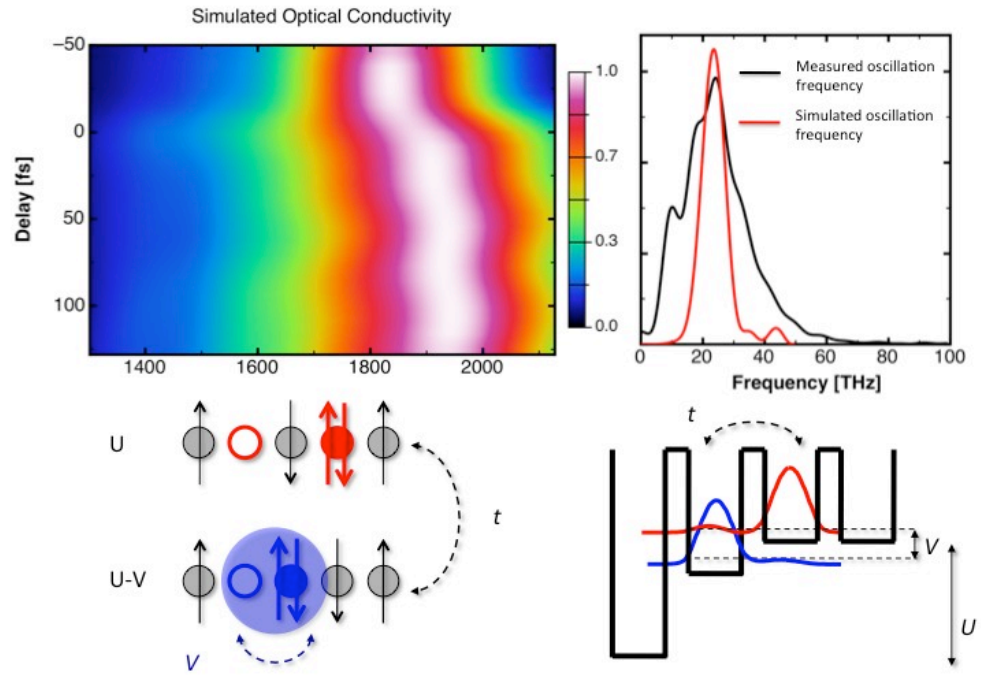


Figure 4

REFERENCES

*corresponding author: andrea.cavalleri@mpsd.cfel.de

these authros have contributed equally to this work

-
- ⁱ M. Imada, A. Fujimori, Y. Tokura *Rev. Mod. Phys.* **70**, 1034 (1998).
- ⁱⁱ T. Hasegawa, S. Kagoshima, T. Mochida, S. Sugiura, Y. Iwasa *Sol State Comm.* **103**, 489 (1997).
- ⁱⁱⁱ T. Hasegawa, T. Mochida, R. Kondo, S. Kagoshima, Y. Iwasa, T. Akutagawa, T. Nakamura, G. Saito *Phys. Rev.* **B62**, 10059 (2000)
- ^{iv} H. Okamoto, H. Matsuzaky, T. Wakabayashi, Y. Takahashi, T. Hasegawa *Phys. Rev. Lett.* **98**, 037401 (2007).
- ^v R. Huber, F. Tauser, A. Brodschelm, M. Bichler, G. Abstreiter, A. Leitenstorfer *Nature* **414**, 286 (2001).
- ^{vi} D. Brida et al. *Opt. Lett.*, **33**, 741 (2008).
- ^{vii} S. Koshihara, Y. Tokura, Y. Iwasa, T. Koda *Phys. Rev. B* **44**, 431 (1991).
- ^{viii} H. Okamoto, K. Ikegami, T. Wakabayashi, Y. Ishige, J. Togo, H. Kishida, H. Matsuzaki *Phys. Rev. Lett* **96**, 037405 (2006).
- ^{ix} A. Cavalleri, Th. Dekorsy, H. Chong, J.C. Kieffer, R.W. Schoenlein *Physical Review B (Rapid Communication)* **70**, 161102(R) (2004)
- ^x F. Schmidt et al. *Science* **321**, 1649 (2008)
- ^{xi} H. J. Zeiger et al. *Phys. Rev. B.* 45 768 (1992)
- ^{xii} N. Strohmaier et al. - arXiv:0905.2963v1 (<http://arxiv.org/abs/0905.2963>)
- ^{xiii} A.L. Cavalieri et al. *Nature* **449**, 1029 (2007)
- ^{xiv} L. Perfetti et al. *Phys. Rev. Lett.* **97**, 067402 (2006)
- ^{xv} A. Cavalleri, M. Rini, H. Chong, T.E. Glover, P.A. Heimann, J.C. Kieffer, R.W. Schoenlein *Physical Review Letters* **95**, 67405 (2005)
- ^{xvi} M. Greiner, O. Mandel, T.W. Haensch, I. Bloch *Nature* **419**, 51 (2002)
- ^{xvii} R. Jordens, N. Strohmaier, K. Guenther, H. Moritz, T. Esslinger *Nature* **455**, 204 (2008)